Conditions for pseudo strain-hardening in fiber reinforced brittle matrix composites

Victor C Li and Hwai-Chung Wu

Advanced Civil Engineering Materials Research Laboratory,
Department of Civil and Environmental Engineering,
University of Michigan, Ann Arbor MI 48109-2125

Apart from imparting increased fracture toughness, one of the useful purposes of reinforcing brittle matrices with fibers is to create enhanced composite strain capacity. This paper reviews the conditions underwhich such a composite will exhibit the pseudo strain-hardening phenomenon. The presentation is given in a unified manner for both continuous aligned and discontinuous random fiber composites. It is demonstrated that pseudo strain-hardening can be practically designed for both types of composites by proper tailoring of material structures.

INTRODUCTION

Pseudo strain-hardening in fiber reinforced composites is associated with the multiple cracking phenomenon of the brittle matrix. To envision this phenomenon, consider a composite specimen subject to uniaxial tensile loading. As the load is increased, a matrix flaw (presumably the largest and oriented normal to the loading direction) may spread over the cross-section of the specimen. The matrix crack may spread stably or unstably, depending on the initial flaw size and the reinforcement details. If spreading is unstable, then a first macroscopic crack is formed in the composite. For an *adequately* reinforced composite, the composite load will be shared by the bridging fibers. These fibers then transfer the load via their interface back into the matrix. If enough load is transferred, the matrix may crack again and the process repeats until the matrix is broken by a series of sub-parallel cracks of approximately equal crack spacing. Straining of the bridging fibers across the matrix cracks and within the matrix blocks give rise to a composite strain that can be substantially higher than the matrix failure strain alone. The importance of this enhanced strain capacity is due to the maintained or even rising composite load during this straining process. Pseudo strain-hardening and multiple cracking have been observed in continuously reinforced ceramic and cement matrices with aligned fibers. Figures 1a,b show the multiple cracking of SiC reinforced glass ceramics (Marshall and Evans, 1985) and Carbon fiber reinforced cement (Akihama et al, 1984). Pseudo strain-hardening and multiple cracking were observed in a random discontinuous polyethylene fiber reinforced cement (Figure 1c, Li and Wu, 1991). The pseudo strain-hardening process and related composite tensile properties have been addressed by a number of investigators (see, e.g. Aveston et al,1971; Marshall et al, 1985,1987; Budiansky et al, 1986; McCartney, 1987; and Mobasher et al, 1991 for continuous aligned fiber reinforced composites, Krenchel and Jensen, 1980; Laws, 1987; Leung and Li, 1989; Li and Leung, 1992; and Li and Wu, 1992 for aligned and randomly oriented discontinuous fiber reinforced composites).

As will be clear from the discussions to follow, it is much more difficult to achieve pseudo strain-hardening in random discontinuous fiber composites compared to continuous aligned ones. However, it is by no means impossible. The challenge is to determine the proper conditions underwhich multiple cracking will occur, despite the reduced efficiency of stress transfer in the random and discontinuous bridging fibers.

For a continuous aligned composite, adequate reinforcement implies that the bridging fibers have substantial number and high enough tensile strength to take over the additional load shed by the cracked matrix. Otherwise, the fibers will rupture resulting in catastrophic brittle type failure. For a random discontinuous fiber composite, adequate reinforcement implies that the bridging fibers have substantial number, high enough bond strength and embedment length (or surface area) to take over the additional load shed by the cracked matrix. Otherwise the fibers will be pulled out resulting in catastrophic brittle type failure. These are the physical limitations we will use for deriving the critical conditions for pseudo strain-hardening in this paper. For short fibers systems, pseudo strain-hardening may also be limited by fiber rupture. However, this case has not been worked out yet.

"Micromechanical modelling of quasi-brittle materials behavior" edited by Victor C Li, ASME Book No AMR118 $60 (members $30)
Appl Mech Rev vol 45, no 8, August 1992

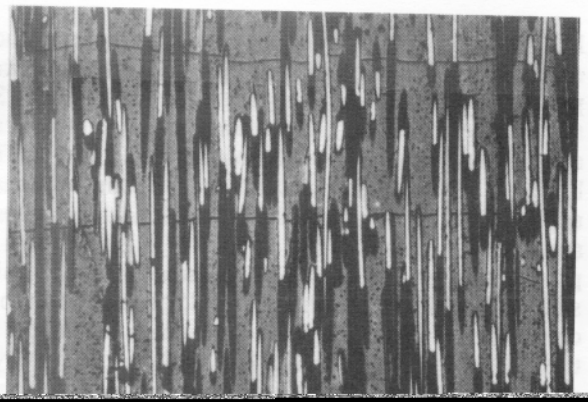

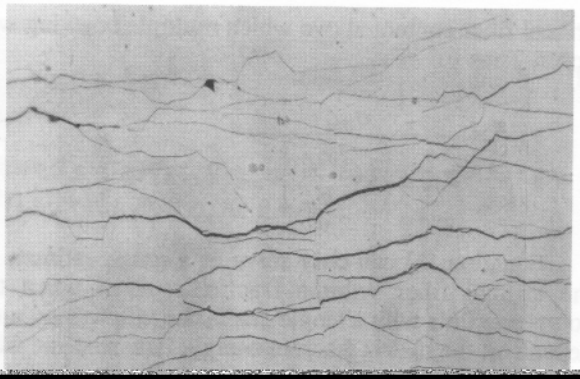

critical fiber content above which multiple cracking will occur. Thus

$$V_f^{crit} = \frac{\sigma_{mu}}{\sigma_{fu} + \left(1 - \frac{E_f}{E_m}\right)\sigma_{mu}} \tag{3}$$

Equation (3) can only serve as a rough estimate of the critical fiber volume fraction. Even when the composite fails with a single crack, the failure load must depend on the matrix fracture energy, flaw size and fiber bridging toughness, rather than just on the matrix failure strain alone (see, e.g. Marshall et al, 1985; Li and Leung, 1992). There is at present no equivalent of eqn.(3) for discontinuous random fiber composites, although the standard procedure for the Rule of Mixture approach would be to introduce efficiency factors to reduce the contribution of fibers from that of the aligned continuous case (see, e.g. Bentur and Mindess, 1990). In the following, we show that the critical fiber volume fraction for pseudo strain-hardening may be expressed in terms of the matrix fracture energy and other fiber and interface related parameters. Indeed, for both continuous or discontinuous systems, we demonstrate in this paper that the critical fiber volume fraction may be interpreted physically as a requirement on the level of toughness induced by fiber bridging as a minimum multiple of the crack tip toughness.

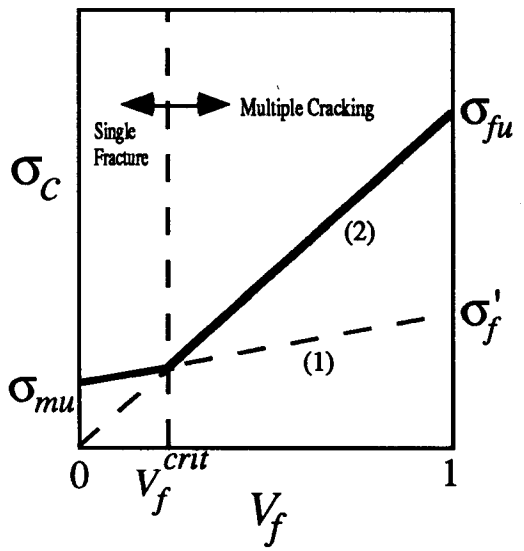

FIG. 2. Condition of multiple cracking for ductile fiber/brittle matrix composites (after Aveston et al, 1971).

SHORT CRACK AND LONG CRACK LIMITS

In the short crack limit (Figure 3a), the crack, while bridged by fibers and therefore requires additional applied load to drive the crack front, behaves essentially like a Griffith crack. Once the net stress intensity factor reaches the crack tip toughness, unstable crack propagation assumes. In the long crack limit (Figure 3b), the crack opening near the crack center asymptotically approaches that of a through-section crack, and the fiber bridging stress there equilibrates with the externally applied load. In this limit, the critical load approaches an asymptotic value. This crack is also known as propagating in a 'self-similar' or 'steady state' fashion, since the stress and deformation fields with respect to the crack tip remains unchanged with crack extension. At this stage, therefore, propagation of the crack front by an amount δc is equivalent to replacing a strip of the loaded composite material far ahead of the crack front by a similar strip far behind the crack front (Figure 4). Such equivalency has been exploited by Budiansky et al (1986) in determination of the steady state tensile strength of aligned continuous fiber composites by considering the energy exchange process in these strips of materials.

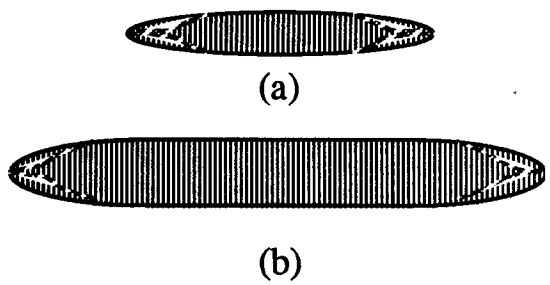

FIG. 3. (a) Short crack with bridging fibers providing closing pressure on crack franks (b) long crack showing crack flattening under steady state condition. Elliptical crack shapes are assumed in the present analysis. The actual crack shape is probably closer to that shown schematically by the dashed lines.

FIRST CRACK STRENGTH

In the short crack limit, the load required to advance the crack front is clearly crack size dependent. The first crack strength may be obtained (Marshall et al, 1985; Li and Leung, 1992) from a consideration of the balance of stress intensity factors associated with the applied load K_L, that with fiber bridging effect K_B and the crack tip fracture toughness K_{tip}:

$$K_L + K_B = K_{tip} \tag{4}$$

For small fiber volume fraction K_{tip} can be taken to be simply the matrix toughness K_m. Otherwise, following Marshall et al (1985), $K_{tip} = (E_c / E_m)K_m$, since the stress intensity factor scales directly with stress. Eqn. (4) may be rewritten as

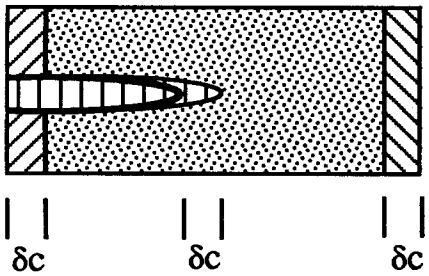

FIG. 4. Crack advance under steady state condition showing a strip of the loaded composite material far ahead of the crack front being replaced by a similar strip far behind the crack front.

$$K_L = K_R \equiv K_{tip} + |K_B| \tag{5}$$

and K_R may be regarded as the enhanced composite toughness due to fiber bridging. (Note that K_B is negative due to closing pressure on crack flanks). McCartney (1987) expressed K_{tip} in terms of K_m differently but coincides with Marshall et al's expression for small V_f. Apart from the work of Miyajima and Sakai (1991), the functional dependence of K_{tip} on K_m and V_f has not been experimentally examined.

K_L scales with the magnitude of the applied load σ and the crack size c, and is given by

$$K_L = 2\sqrt{\frac{c}{\pi}}\sigma \tag{6}$$

where the penny shaped crack configuration (in an infinite body) has been assumed. The magnitude of K_B is expected to depend on the details of the fiber bridging effect. Treating K_B as due to applied traction σ_B acting on the crack flanks at radial distance r from the center, K_B may be expressed via superposition as

$$K_B = -2\sqrt{\frac{c}{\pi}}\int_0^1 \sigma_B[\delta(R)]\frac{RdR}{\sqrt{1-R^2}} \tag{7}$$

The traction σ_B is written as a functional of crack opening δ because the smeared out bridging stress of fibers varies with the amount of crack opening, and δ in turns depends on the radial distance r from the crack center. In (7), $R=r/c$. The bridging stress will first increase until some critical crack opening, then decrease due to fiber breakage and/or pull-out.

The bridging stresses, σ_B, have been theoretically derived based on frictional debonding of the interface for continuous aligned (hereafter designated as CA), (Marshall et al, 1985) and for discontinuous random (hereafter designated as DR) composites (Li and Leung, 1992). These normalized stresses can be expressed in a generalized form, which leads to

$$\tilde{\sigma}_B = g\left[C_0\left(\tilde{\delta}/\tilde{\delta}^*\right)^{1/2} - C_1\tilde{\delta}/\tilde{\delta}^*\right] \qquad \tilde{\delta} \le \tilde{\delta}^* \tag{8}$$

where $\tilde{\sigma}_B = \sigma_B/\sigma_o$; $\sigma_o = C_2 V_f \tau (L_e/d_f)$; $\tilde{\delta} = \delta/(L_e/2)$; $\tilde{\delta}^* = 2\tau/[(1+\eta)E_f](L_e/d_f)$; $\eta = V_f E_f / V_m E_m$, and

$$L_e = \begin{cases} 2L_c & \text{CA} \\ L_f & \text{DR} \end{cases}$$

where d_f is the fiber diameter, L_f is the discontinuous fiber length, and L_c the critical embedment length ($=\sigma_{fu}d_f/4\tau$). σ_{fu} is the fiber ultimate strength, assumed uniform and deterministic, and τ is the fiber/matrix interface frictional bond strength. The constants C_0, C_1 and C_2 are tabulated in Table 1 for the CA and DR cases. From hereon, all constants C_i with different values for CA and DR can be found in Table 1. The mechanical influence of fiber orientation is also explicitly considered, expressed as the snubbing factor, g (Li et al, 1990). Typically, g values are equal or greater than unity for DR cases, whereas g equals one (no snubbing effect) for CA composites. σ_o may be interpreted as the maximum fiber bridging stress of the composite. Eqn (8) expresses a spring-like relationship between the traction and opening displacement across the crack faces at any point in the wake of the crack front.

In general in the presence of fiber bridging, the crack opening δ is not known *a priori* as a function of position R, and evaluation of K_B typically requires an iterative process (see Marshall, 1985). For simplicity, the crack profile is assumed to take on the same elliptical shape (Figure 3) as that for a crack with uniform cohesive traction (see, e.g. Brock, 1986), so that

$$\tilde{\delta} = \sqrt{\tilde{c}\left(1-R^2\right)} \tag{9}$$

where $\tilde{c} = c/c_0$ and $c_0 = \left[\frac{E_c L_e}{2K_{tip}}\right]^2 \frac{\pi}{16\left(1-\nu^2\right)^2}$

The first crack strength σ_{fc} may be obtained when equation (4) is satisfied, and making use of (6), (7), (8) and (9):

$$\tilde{\sigma}_{fc}/g = \frac{\sqrt{\pi}}{2}\frac{\overline{K}}{\overline{c}} + \left[C_3\sqrt{\overline{c}} - C_4\overline{c}\right] \tag{10}$$

where $\overline{K} = \frac{K_{tip}}{g\sigma_0\sqrt{c_0\tilde{\delta}^*}}$, $\overline{c} = \sqrt{\tilde{c}}/\tilde{\delta}^*$

Equation (10) depicts the first cracking strength resulting from a combination of crack tip fracture resistance (represented by the 1st term on the right hand side) and fracture resistance associated with fiber bridging (represented by the 2nd term in square brackets of the right hand side). This equation remains valid as long as the crack shape maintains elliptical as the bridging zone grows.

CONDITIONS FOR PSEUDO STRAIN-HARDENING

From the discussion relating to short and long crack limits, it is clear that the short crack limit is associated with first crack strength which is crack size dependent, whereas the long crack limit is associated with the steady state crack strength which is independent of crack size. The transition from short to long crack limit occurs when the bridging stress in the center of the (short) crack becomes equal to the applied load. Further crack length extension will be under the steady state condition. This is illustrated in Figure 5, which shows the first crack strength (eqn. 10) and the fiber bridging stress (eqn. 8) plotted as a function of crack size.

The above consideration leads to a transitional crack size c_s, which satisfies

$$\tilde{\sigma}_B\left(\tilde{\delta}_m\right)=\tilde{\sigma}_{fc} \tag{11}$$

where the opening in the crack center (R =0) is given by $\tilde{\delta}_m=\sqrt{\tilde{c}}$ from (9). Using (8) and (10) in (11) leads to

$$\bar{K}=\frac{2}{\sqrt{\pi}}\bar{c}_s\left(C_5\sqrt{\bar{c}_s}-C_6\bar{c}_s\right) \qquad 0\le\bar{c}_s\le 1 \tag{12}$$

Eqn (12) defines the magnitude of $\bar{c}_s$ ($\equiv\sqrt{c_s/c_0}/\tilde{\delta}^*$) for any given value of $\bar{K}$. However, $\bar{c}_s$ cannot exceed unity since the bridging stress is either decreasing (for short fibers being pulled out) or zero (for continuous fibers being ruptured) for $\bar{c}_s$ > 1 (Li and Leung, 1992). This puts an upper limit on the value of $\bar{K}$. From (12) the critical values of $\bar{K}$ ($\bar{K}^{crit}$) are determined to be 0.188 for random discontinuous fiber composites and 0.376 for continuous aligned fiber composites. Above $\bar{K}^{crit}$, no pseudo strain-hardening occurs, and the composite fails catastrophically with a single large fracture. Thus, for design of composites with enhanced strain capacity, it is important to ensure a $\bar{K}$ value below $\bar{K}^{crit}$.

The $\bar{K}^{crit}$ condition for pseudo strain-hardening may be translated into physically meaningful requirement of the fracture toughness induced by fiber interfacial debonding G_r (Appendix 1):

$$\bar{K}=\begin{cases}\dfrac{8}{3\sqrt{\pi}}\dfrac{G_{tip}}{G_r}\\[2ex] \dfrac{10}{3\sqrt{\pi}}\dfrac{G_{tip}}{G_r}\end{cases}\le\bar{K}^{crit}=\begin{cases}\dfrac{2}{3\sqrt{\pi}} & \text{CA}\\[2ex] \dfrac{1}{3\sqrt{\pi}} & \text{DR}\end{cases} \tag{13}$$

Thus

$$\frac{G_r}{G_{tip}}\ge\begin{cases}4 & \text{CA}\\ 10 & \text{DR}\end{cases} \tag{14}$$

Eqn (14) expresses the need for high bridging toughness relative to crack tip toughness for pseudo strain-hardening. It implies the requirement of sufficient energy absorption through frictional work at the fiber/matrix interface. For design applications, it is useful to re-express (14) in terms of the critical fiber volume fraction:

$$V_f\ge V_f^{crit}\equiv\frac{C_7G_{tip}}{\tau d_f\left(\dfrac{L_e}{d_f}\right)^2\tilde{\delta}^*} \tag{15}$$

Equation (15) then replaces (3) which is based on the Rule of Mixture. Note that (14) and (15) clearly reflects the importance of the crack tip and therefore the matrix toughness in the condition for pseudo strain-hardening. The required fiber volume fraction increases for a matrix of higher fracture toughness. It may therefore be expected that pseudo strain-hardening in ceramic matrix composites will be more difficult to achieve when compared to cementitious matrixes because of the higher inherent matrix toughness in ceramics.

Table 1: Constants used in the generalized form for CA and DR cases.

	C_0	C_1	C_2	C_3	C_4	C_5	C_6	C_7	C_8	C_9
CA	1	0	2	2/3	0	1/3	0	6	1	0
DR	2	1	1/2	4/3	1/2	2/3	1/2	48/g	2g	g

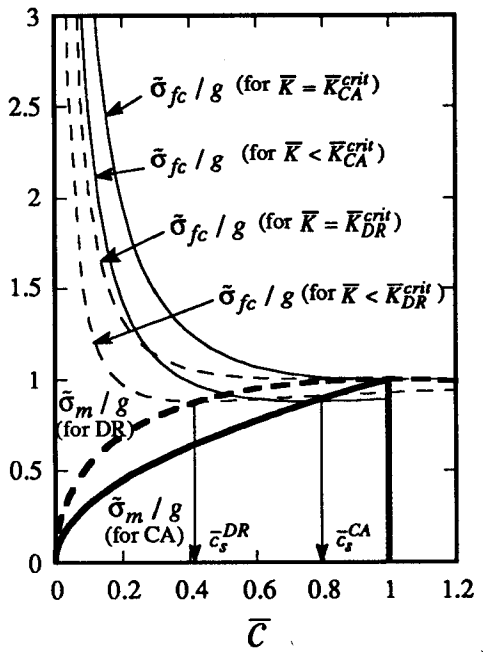

FIG. 5. First crack strength and bridging stress at crack center. Conditions for steady state cracking require these curves to meet, i.e. for both continuous aligned (solid lines, labeled CA) and discontinuous random (dashed lines, labeled DR) fiber composites.

It is interesting to note that while $\bar{K}^{crit}$ (or eqn. (14) and (15)) defines the necessary condition for achieving pseudo strain-hardening, sufficiency is not guaranteed. In fact, Figure 5 shows that for initial crack size below c_s, the first crack strength can be higher than the maximum fiber bridging stress (i.e. $\sigma_{fc}/g > \sigma_0$ or $\tilde{\sigma}_{fc}/g > 1$). In that case, the spreading of the matrix crack is accompanied by fiber breakage for aligned continuous fiber composites and fiber pull out for random discontinuous fiber composites. This implies that pseudo strain-hardening must occur if the initial crack size is larger than c_s, in addition to the requirement expressed through eqn. (14) or (15) (Actually, there is a small range of $c < c_s$, for which multiple cracking is guaranteed, see Li and Leung, 1992).

From (15), it would seem like that for any given τ and L_e/d_f, a V_f^{crit} can be computed. Unfortunately, this is not the case. This is because G_r does not increase monotonically with V_f (see Figure 6). [Note that G_r scales with $V_f\tilde{\delta}^*$, and $\tilde{\delta}^*$ scales with $(1\text{-}V_f)$, see Appendix 1]. At high fiber volume fraction, despite higher bridging stress, the amount of crack opening $\tilde{\delta}^*$ and therefore frictional work is in fact reduced, so that eqn. (14) is not guaranteed to be satisfied. The auxiliary condition may be obtained by requiring (15) to yield a real solution for V_f, leading to

$$A \le \begin{cases} \dfrac{\sigma_{fu}^3}{\tau} & \text{CA} \\ \tau^2\left(L_f/d_f\right)^3 & \text{DR} \end{cases} \tag{16}$$

where $A \equiv \dfrac{24\left(1-\nu^2\right)E_f(1+\eta)K_m^2E_c}{E_m^2 d_f V_f' g}$, and V_f' must satisfy the following equation:

$$V_f'\left[E_c\left(E_f-E_m\right)+(1+\eta)V_m' E_m\frac{\partial E_c}{\partial V_f'}\right] = (1+\eta)E_mE_c\left(1-2V_f'\right) \tag{17}$$

For CA composites, using Rule of Mixture for E_c, (16) can be reduced to

$$\frac{\sigma_{fu}^3}{\tau} \ge \frac{96E_f^2K_m^2}{E_m^2 d_f} \tag{18}$$

In the case of random discontinuous fiber composites, (16) puts a lower limit on fiber aspect ratio and interfacial bond. In the case of continuous aligned fiber composites, (16) puts a lower limit on fiber strength and upper limit on interfacial bond.

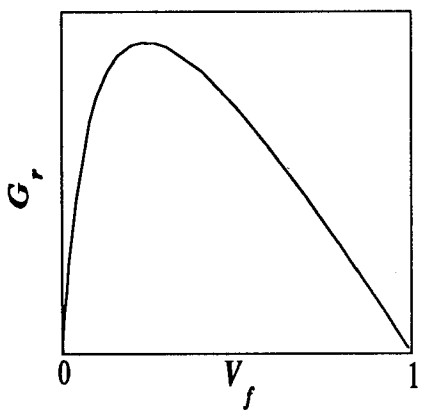

FIG. 6. Schematic representation of frictional debonding energy vs fiber volume fraction.

STEADY STATE CRACK STRENGTH

The steady state crack strength may be obtained by evaluating the first crack strength (eqn. 10) at the transitional crack size (Li and Leung, 1992), i.e.

$$\tilde{\sigma}_{ss} = \tilde{\sigma}_{fc}(\bar{c} = \bar{c}_s) = C_8\sqrt{\bar{c}_s} - C_9\bar{c}_s \quad (19)$$

where $\bar{c}_s$ has been defined in terms of $\bar{K}$ in (12). From the above discussion, the steady state crack strength corresponds to the load bearing capacity in the long crack limit and is therefore always smaller than the first crack strength when $c < c_s$. These strength properties have been computed assuming for convenience that the crack shape remains elliptical, even in the presence of the fiber bridging effect. More accurate numerical computations without such an assumption show that the steady state crack strength for continuous aligned fiber composites is overestimated by about 20% (Marshall, 1985). Apart from this numerical difference, Eqn (19) reproduces the results of Aveston et al (1971) and Marshall et al (1985) for the case of continuous aligned fiber composites, and those of Li and Leung (1992) for the case of discontinuous random fiber composites.

A DESIGN EXAMPLE

Eqns (15) and (16) provide design rules for pseudo strain-hardening. It turns out that even for random discontinuous fiber composites, high fiber volume fraction is not necessarily an absolute requirement, provided other parameter combinations are chosen properly. This concept is demonstrated with a cement matrix reinforced with random discontinuous polymer fibers.

As revealed in equation (15), low matrix toughness and high aspect ratio are in favor of low critical fiber volume fraction necessary for multiple cracking. In addition, equation (16) should also be satisfied in order to yield a real solution of eqn (15). A high modulus polyethylene fiber (Spectra fiber, Allied Corporation) and low toughness cement paste are selected for a model composite to test the validity of (15) and (16). Table 2 summarizes the micromechanical parameters used in this system. Detailed descriptions and experimental procedure will be presented in a separate paper (Wu and Li, 1992). V_f^{crit} is computed to be as low as 0.3% by volume. As shown in Figure 7, similar to the matrix alone, the composite with V_f=0.1% demonstrates a catastrophic failure. In contrast to this, the composite of V_f=1% shows a significant ductility as well as enormous fracture toughness. Clear sub-parallel cracks were recorded from the specimen surface, as shown in Figure 1c.

In Table 3 the first cracking strength, σ_{fc}, and steady state strength, σ_{ss}, of discontinuous random Spectra fiber reinforced cement with four different fiber volume fractions are summarized. Two different values of snubbing factor are used. Limited data are published for polypropylene fiber (g=1.78) and nylon fiber (g=2.31) (Li et al, 1990). When snubbing effect is inactive, g resumes one. The actual strength improvements are found to be less than predicted. This is perhaps due to increasing difficulty in uniform mixing and poor workability as V_f increases. On the other hand, if the predicted steady state strength σ_{ss} is reduced by 20% due to the crack shape effect discussed earlier, they would be reasonably close to the experimentally measured values. As expected, significant ductility improvements were found for the three composites with $V_f > V_f^{crit}$ (Figure 8). The ultimate strain ε_{cu} for the composites with pseudo strain-hardening is approximately 220 times that of those without strain-hardening.

DISCUSSIONS AND CONCLUSIONS

This paper reviews the conditions under which brittle matrixes such as cement and ceramics can be made to behave more like metallic materials which exhibit strain-hardening when loaded beyond the yield point. These conditions are derived in a unified manner for both continuous and discontinuous fiber composites. The physical interpretations of the necessary and sufficient

Table 2: Micromechanical parameters used in this study.

Fiber	d_f (μm)	L_f (mm)	E_f (GPa)	Matrix	E_m (GPa)	K_m (MPa$\sqrt{m}$)	τ (MPa)	V_f^{crit} (%)
Spectra	38	12.7	120	OPC paste	15	0.2	1.0	0.3

Table 3: First cracking and steady state strengths of Spectra fiber reinforced cement.

V_f (%)	σ_{fc} (MPa)			σ_{ss} (MPa)		
	Expt	Pred		Expt	Pred	
		g=1	g=2		g=1	g=2
0	1.6	-	-	-	-	-
0.1	1.7	1.68	1.74	-	-	-
1	-	-	-	2.2	1.5	2.4
2	-	-	-	2.4	2.5	4.1
3	-	-	-	2.5	3.4	5.6

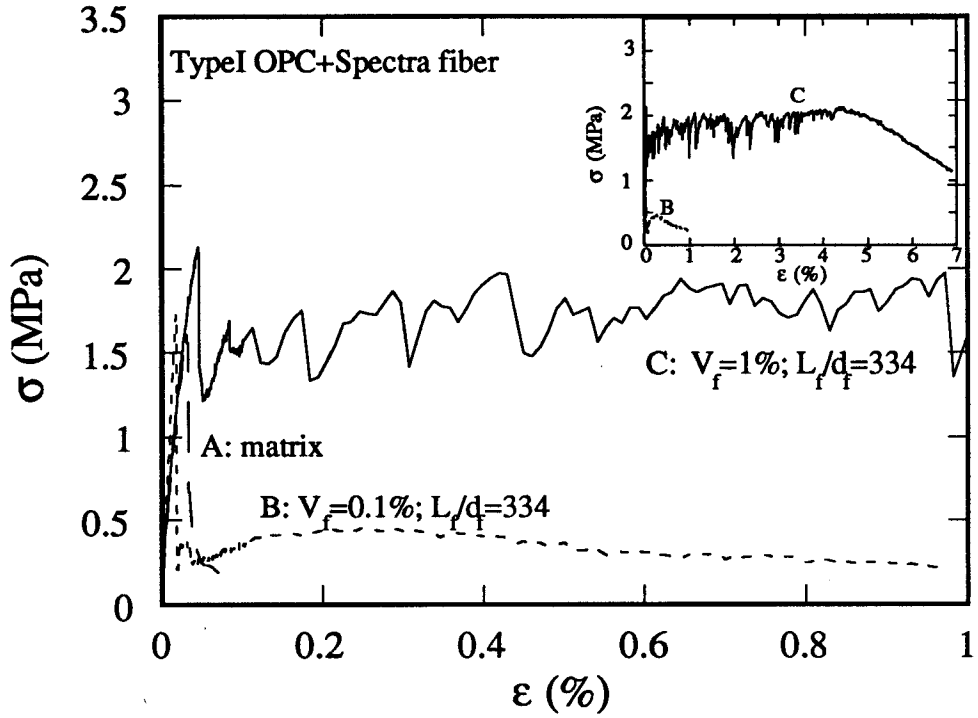

FIG. 7. Experimental stress-strain curves for discontinuous random Polyethylene fiber reinforced cement with various fiber volume fraction. Insert shows complete curves.

conditions for pseudo strain-hardening are highlighted. Specifically, the analyses reveal the importance of the G_r/G_{tip} ratio, for both the CA and DR cases. The conditions (eqn. 14,15) discussed in this paper, based on fracture mechanics principles, are dramatically different from those obtainable from the Rule of Mixture (eqn 3). In addition, auxiliary conditions (eqn 16) on fiber strength, bond properties and aspect ratio, not considered in previous works, are now revealed.

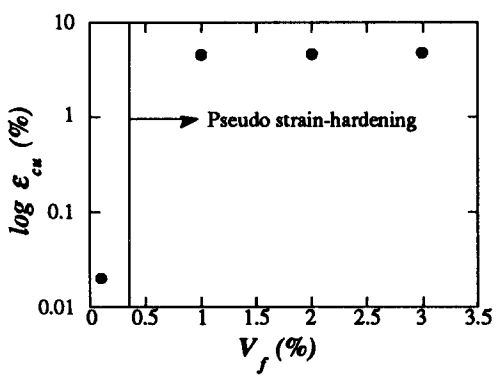

FIG. 8. Significant ductility achieved when $V_f > V_f^{crit}$ (V_f^{crit}=0.3%) for discontinuous random Polyethylene fiber reinforced cement.

Eqn (16) is the necessary condition for achieving multiple cracking. When this condition is violated, (14) and (15) cannot be satisfied regardless of V_f. This implies that for very high fiber volume fraction, pseudo strain-hardening can in fact be suppressed even though the composite strength may begin to approach the maximum bridging strength σ_o of the reinforcing fibers. Future experimental investigation is necessary to confirm this observation.

Eqn (15) suggests that V_f^{crit} can be much higher for DR than for CA composites. As an example, for the same Spectra fiber/OPC paste, used in this paper, V_f^{crit} is only 0.001% for CA (σ_{fu}=2600 MPa) versus 0.3% for DR composites. For a typical steel fiber used in cement reinforcement (E_f=200 GPa, τ =5 MPa, d_f=250 μm, L_f =12 mm, σ_{fu} =600 MPa, K_m =.4 MPa$\sqrt{m}$, and E_m =20 GPa), V_f^{crit} is 0.4% for CA versus 9% for DR composites. Hence adequate reinforcement for pseudo strain-hardening is more readily achieved for CA composites, as reflected in the literature where evidence is abundant. Nevertheless, with proper design, pseudo strain-hardening is also achievable for DR composites, as demonstrated in this paper.

The discussions in this paper have been based on simple fiber/matrix interaction models. However the formulation is general enough that it can be extended via

modification of the $\sigma(\delta)$ relationship to include, for example, interfacial elastic bond, and elastic mismatch between fibers and matrix.

Although pseudo strain-hardening data for discontinuous random fiber composites are limited, the consistency between results for continuous and discontinuous systems, and the demonstration with Spectra FRC discussed in this paper, lend confidence to designing discontinuous fiber reinforced brittle matrix composites with enhanced strain-capacity.

ACKNOWLEDGMENT

This research has been supported by a research grant from the National Science Foundation (Program manager: Dr. K. Chong) to the University of Michigan, Ann Arbor. Comments by D. Marshall and S. Shah led to many useful improvements in this manuscript. Photo courtesy of Dr. D. Marshall (Fig 1a) and Dr. S. Akihama (Fig 1b) are gratefully acknowledged.

REFERENCES

Akihama S, Suenaga T, and Banno T (1984) *Mechanical Properties of Carbon Fiber Reinforced Cement Composite and the Application to Large Domes*, Kajima Institute of Construction Technology, KICT Report NO. 53, Tokyo, Japan.

Aveston J, Cooper GA, and Kelly A (1971). Single and Multiple Fracture, *in the Properties of Fiber Composites, Conf. Proc.*, IPC Science and Technology Press Ltd., 15-24.

Bentur A and Mindess S (1990). *Fiber Reinforced Cementitious Composites*, Elsevier Applied Science.

Brock D (1986). *Elementary Engineering Fracture Mechanics*, 4th Edition, Martinus Nijhoff Publishers.

Budiansky B, Hutchinson JW, and Evans AG (1986). Matrix Fracture in Fiber-Reinforced Ceramics, *J. Mech. Phys. Solids* Vol. 34, no. 2, 167-189.

Krenchel H and Jensen HW (1980). Organic Reinforcing Fibers for Cement and Concrete, in Fibrous Concrete, The Concrete Society, *Proceeding of the Symposium on Fibrous Concrete*, Lancaster, The Construction Press.

Laws V (1987). Stress/Strain Curve of Fibrous Composites, *J. Mater. Sci. Letters*, 6, 675-678.

Leung CKY and Li VC (1989). First-Cracking Strength of Short-fiber Reinforced Ceramics, *Ceramics Eng. Sci. Proc.*, 9/10, 1164-1178.

Li VC and Leung CKY (1992). Theory of Steady State and Multiple Cracking of Random Discontinuous Fiber Reinforced Brittle Matrix Composites", accepted for publication in *ASCE J. of Engng. Mechanics*.

Li VC and Wu HC (1992) Pseudo Strain-Hardening Design in Cementitious Composites, in *Proc. of International Workshop on High Performance Fiber Reinforced Cement Composites*, Ed. H. Reinhardt and A. Naaman, Chapman and Hall, 371-387.

Li VC, Wang Y, and Backer S (1990) Effect of Inclining Angle, Bundling, and Surface Treatment on Synthetic Fiber Pull-out from a Cement Matrix, *Composites*, Vol. 21, 2, 132-140.

Marshall DB and Evans AG (1985). Failure Mechanisms in Ceramic-Fiber/Ceramic-Matrix Composites, *J. Am. Ceram. Soc.*, Vol. 68, No. 5, 225-231.

Marshall DB, Cox BN, and Evans AG (1985). The Mechanics of Matrix Cracking in Brittle-Matrix Fiber Composites, *Acta Metall.* Vol.33, no. 11, 2013-2021.

Marshall DB and Cox BN (1987). Tensile Fracture of Brittle Matrix Composites: Influence of Fiber Strength, *Acta Metall.* Vol.35, no.11, 2607-2619.

McCartney LN (1987). Mechanics of Matrix Cracking in Brittle-matrix Fiber-reinforced Composites, *Proc. R. Soc. London*, A 409, 329-350.

Miyajima T and Sakai M (1991). The Fracture Toughness for First Matrix Cracking of a Unidirectionally Reinforced Carbon/Carbon Composite Material, *J. Mater. Res.* Vol. 6, No. 11.

Mobasher B, Ouyang C, and Shah SP (1991). Modeling of Fiber Toughening in Cementitious Materials using an R-Curve Approach, *Int'l J. of Fracture*, 50, 199-219.

Wu HC and Li VC (1992), in preparation.

Appendix 1: Derivation of frictional debonding energy, G_r

The fracture energy due to fiber frictional debonding can be computed from

$$G_r = \int_0^{\delta^*} \sigma_B(\delta)\,d\delta \tag{A1}$$

where σ_B is given by eqn (8), and δ^* is the maximum crack opening at maximum bridging stress. Thus

$$G_r = \begin{cases} \dfrac{2}{3}\tau V_f d_f \left(\dfrac{L_e}{d_f}\right)^2 \tilde{\delta}^* & \text{CA} \\ \dfrac{5}{24} g\tau V_f d_f \left(\dfrac{L_f}{d_f}\right)^2 \tilde{\delta}^* & \text{DR} \end{cases} \tag{A2}$$